



# Laurentide Ice Sheet persistence during Pleistocene interglacials

Danielle E. LeBlanc<sup>1</sup>, Jeremy D. Shakun<sup>1</sup>, Lee B. Corbett<sup>2</sup>, Paul R. Bierman<sup>2</sup>, Marc W. Caffee<sup>3</sup> and Alan J. Hidy<sup>4</sup>

<sup>1</sup>Department of Earth and Environmental Sciences, Boston College, Chestnut Hill, Massachusetts 02467, USA

<sup>2</sup>Rubenstein School of the Environment and Natural Resources, University of Vermont, Burlington, Vermont 05405, USA

<sup>3</sup>Department of Physics and Astronomy and Department of Earth, Atmospheric, and Planetary Sciences, Purdue University, West Lafayette, Indiana 46202, USA

<sup>4</sup>Center for Accelerator Mass Spectrometry, Lawrence Livermore National Laboratory, Livermore, California 94550, USA

## ABSTRACT

While there are no ice sheets in the Northern Hemisphere outside of Greenland today, it is uncertain whether this was also the case during most other Quaternary interglacials. We show, using *in situ* cosmogenic nuclides in ice-rafted debris, that the Laurentide Ice Sheet was likely more persistent during Quaternary interglacials than often thought. Low  $^{26}\text{Al}/^{10}\text{Be}$  ratios (indicative of burial of the source area) in marine core sediment suggest sediment source areas experienced only brief (on the order of thousands of years) and/or infrequent ice-free interglacials over the past million years. These results imply that complete Laurentide deglaciation may have only occurred when climate forcings reached levels comparable to those of the early Holocene, making our current interglacial unusual relative to others of the mid-to-late Pleistocene.

## INTRODUCTION

Since the start of the Pleistocene Epoch (ca. 2.6 Ma), continental ice sheets have ebbed and flowed over glacial-interglacial cycles across North Atlantic landscapes. A long-standing question is to what extent were past interglacials like that of today. Did Northern Hemisphere ice sheets outside Greenland always disappear, as in the Holocene, or did remnant ice domes survive during interglacials? The former scenario would suggest a low deglaciation threshold where the conditions required for ice disappearance were reached during most or all Pleistocene interglacials. The latter scenario would suggest that ice sheets only fully disappear when multiple factors conspire for long enough to drive complete deglaciation (Ullman et al., 2015).

Understanding the history of the Laurentide Ice Sheet is of particular interest because it was the last Northern Hemisphere ice sheet to deglaciate during the Holocene and is key to determining whether past interglacials reached ice-free conditions outside of Greenland. Reconstructing Laurentide margins prior to the Last Glacial Maximum is difficult due to the limitations of traditional geologic records. Terrestrial records are discontinuous due to their removal by glacial erosion. Benthic  $\delta^{18}\text{O}$  provides a continuous record of ice-volume changes (Lisiecki and Raymo, 2005), but it is difficult to link to

a specific ice sheet; the isotope signal is also confounded by an uncertain ocean temperature component and may not be a reliable recorder of ice volume (Dalton et al., 2022). The presence of ice-rafted debris in marine sediments indicates times with large, marine-terminating ice sheets, but ice-rafted debris cannot constrain the extent of retreat when ice margins fall short of coastlines. Given these limitations, reconstructions of Laurentide margins during Pleistocene interglacials have only been produced for the last interglacial and have large ranges from no ice to sizable ice domes spanning much of Canada (Fig. 1; Kleman et al., 2010; Batchelor et al., 2019; Miller et al., 2022).

## METHODS

We assessed Laurentide Ice Sheet persistence during past interglacials by measuring concentrations of cosmogenic  $^{10}\text{Be}$  and  $^{26}\text{Al}$  in quartz sand across North Atlantic Heinrich layers (layers rich in ice-rafted debris from Laurentide discharge episodes during the last glacial period). Cosmogenic nuclides in ice-rafted debris record an integrated exposure, burial, and erosion history of the regions from which sediment was sourced. During ice-free times, nuclides accumulate in quartz within rock and sediment exposed to cosmic radiation. Nuclide production via spallation reactions is highest at the surface ( $\sim 4$  atoms  $\text{g}^{-1}$

$\text{yr}^{-1}$  at high latitudes for  $^{10}\text{Be}$ ;  $7.3x$  higher for  $^{26}\text{Al}$ ) and rapidly attenuates with depth, but low levels of production ( $<10^{-1}$  atoms  $\text{g}^{-1} \text{yr}^{-1}$ ) by muons extend several tens of meters into the subsurface (Gosse and Phillips, 2001).

During times of significant ice-sheet cover, most nuclide production halts because surface materials are shielded from cosmic rays. Because  $^{26}\text{Al}$  ( $t_{1/2} = 0.7$  m.y.) decays more rapidly than  $^{10}\text{Be}$  ( $t_{1/2} = 1.4$  m.y.), the  $^{26}\text{Al}/^{10}\text{Be}$  ratio decreases below the production value during intervals of burial longer than  $\sim 10^5$  yr. The long half-lives of  $^{10}\text{Be}$  and  $^{26}\text{Al}$ , and their accumulation many meters into the subsurface by muonic production, mean they are well suited to retain a memory of near-surface process history over Pleistocene time scales, even in areas with deep erosion (Briner et al., 2016).

Glacial erosion removes heavily irradiated material from the surface and exhumes progressively nuclide-poorer material at depth. Glacial sediment is derived primarily from warm-based, erosive sectors of an ice sheet; thus, cosmogenic nuclide data provide information about ice-sheet behavior in sediment-generating regions. Although the ice-rafted debris we analyzed was transported to the ocean by marine-terminating ice during the last glacial period, cosmogenic nuclides in ice-rafted debris reflect prior exposure, burial, and erosion in the sediment source areas.

We made 26 paired cosmogenic nuclide measurements from Heinrich layers 1 through 6 (H1–H6, 17–60 ka), as well as intervening layers, at core sites on the west and east sides of the North Atlantic Ocean (Fig. 1). To obtain enough quartz sand for measurement ( $>5$  g), multiple subsamples were amalgamated from each layer. Western core sites (Integrated Ocean Drilling Program [IODP] Sites U1302 and U1303 at  $50.2^\circ\text{N}$ ,  $45.6^\circ\text{W}$  and  $50.2^\circ\text{N}$ ,  $45.7^\circ\text{W}$ , and EW9302-2JPC at  $48.8^\circ\text{N}$ ,  $45.1^\circ\text{W}$ ) sit at the

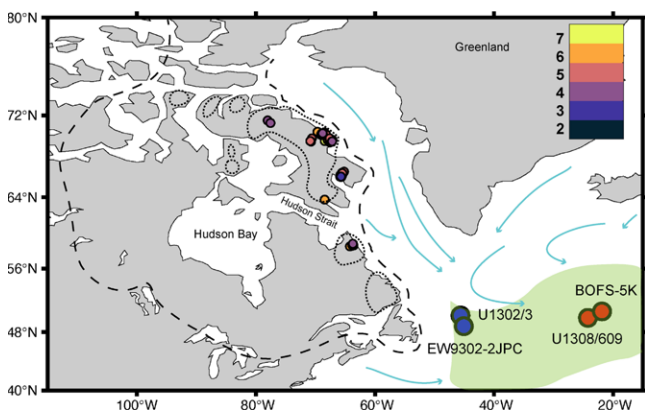


**Figure 1. Cores analyzed in this study and  $^{26}\text{Al}/^{10}\text{Be}$  ratios (scale bar at top right) in terrestrial bedrock from prior studies (Miller et al., 2006; Briner et al., 2006, 2014; Corbett et al., 2016). Also shown are the last glacial ice-rafted debris belt (light green), maximum and minimum estimates of the Laurentide Ice Sheet extent at 95 ka (black dashed and dotted lines; Dalton et al., 2022), and modern ocean currents (arrows).**

mouth of the Labrador Sea and received icebergs predominantly from eastern Canada via the Labrador Current (Mao et al., 2014; Fendrock et al., 2022). Eastern core sites (BOFS-5 K at 50.7°N, 21.9°W, Deep Sea Drilling Project [DSDP] Site 609 at 49.9°N, 24.2°W, and IODP Site U1308, a reoccupation of Site 609) lie just east of the Mid-Atlantic Ridge within the last-glacial ice-rafted-debris belt (Ruddiman, 1977) at the confluence of iceberg pathways from the Laurentide, Greenland, and European ice sheets (Grousset et al., 1993; Bond and Lotti, 1995; Bigg et al., 2011).

All Heinrich layers on the western side of the basin and H1, H2, H4, and H5 in the east contain detrital carbonate, which has been traced to the Hudson Strait sector of the Laurentide Ice Sheet (Hemming, 2004). Because we analyzed quartz rather than carbonate, samples from these Heinrich layers came largely from surrounding silicate terranes upflow of the Hudson Strait ice stream, which drained a large portion of the Laurentide Ice Sheet. Previous provenance work supports this interpretation and shows that Heinrich layers contain predominantly Paleoproterozoic-aged grains with some younger and older grains, suggesting sediments came from large sectors of northeastern Canada and perhaps Greenland (Hemming et al., 1998; Hemming and Hajdas, 2003). Conversely, intervening layers have a greater number of younger and older grains, especially in eastern North Atlantic samples, indicating contribution from additional sources such as southeastern Canada in the west and Europe in the east during non-Heinrich times (see the Supplemental Material<sup>1</sup>).

## RESULTS

The  $^{10}\text{Be}$  concentrations decrease through time in western samples but are variable in east-

ern samples, which we attribute to differences in sediment provenance. The smooth decline in  $^{10}\text{Be}$  concentrations of western samples over time, across both Heinrich and non-Heinrich intervals, is consistent with sediment supplied by erosion and excavation under a single, persistent ice-sheet sector, which we infer was part of the Laurentide Ice Sheet. Western sample  $^{10}\text{Be}$  concentrations are low,  $\sim 7000$ – $19,000$  atoms  $\text{g}^{-1}$  (i.e., less than half the value expected from 10 k.y. of interglacial surface exposure [ $\sim 40,000$  atoms  $\text{g}^{-1}$ ]). Such low concentrations imply that sediment with the highest nuclide concentration following last interglacial exposure was removed by erosion earlier in the glacial period and that the ice-rafted debris we

measured was sourced primarily from areas of deep subglacial erosion.

We attribute the generally higher, more variable  $^{10}\text{Be}$  concentrations in eastern samples to a mixture of sources, which agrees well with earlier provenance work (see Supplemental Material). During H1, H2, H4, and H5,  $^{10}\text{Be}$  concentrations in the east are indistinguishable from those in the west, suggesting Laurentide-derived icebergs (and the sediments they carried) were distributed across the North Atlantic Ocean basin. The  $^{10}\text{Be}$  concentrations are higher in H3 and H6 in the east relative to the west and similar to concentrations in eastern background intervals (times between Heinrich events). These patterns suggest that Laurentide iceberg discharges were smaller during H3 and H6, carried less ice-rafted debris, and/or melted before reaching the east (Bond et al., 1992; Gwiazda et al., 1996).

The  $^{26}\text{Al}/^{10}\text{Be}$  ratios (3.4–5.9) are substantially below the high-latitude surface production ratio ( $\sim 7.3$ ) in all samples, indicating the ice-rafted debris records lengthy Pleistocene histories dominated by burial (Fig. 2A). Laurentide-derived samples (all western samples and samples H1, H2, H4, and H5 in the east) have a mean ratio of 4.7, which requires a minimum of 900 k.y. of decay following initial exposure, assuming the sand we analyzed experienced a single exposure event followed by burial. If the sediment experienced multiple alternating episodes of exposure and burial, then the total burial time must have been even longer because

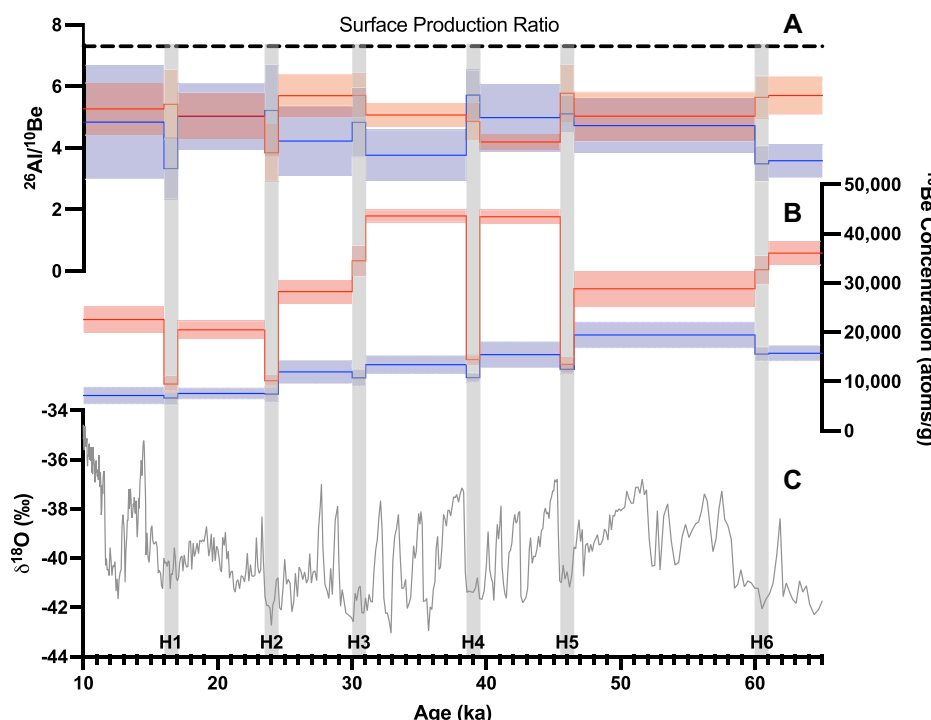


**Figure 2. Measured  $^{26}\text{Al}/^{10}\text{Be}$  ratios (A) and  $^{10}\text{Be}$  concentrations (B) in ice-rafted debris from the western (blue) and eastern (red) North Atlantic cores. Shading shows  $1\sigma$  uncertainty. (C) Greenland Ice Sheet Project 2 (GISP2)  $\delta^{18}\text{O}$  shown as a proxy for Greenland temperature (Grootes and Stuiver, 1999). Heinrich layers are indicated by gray bars.**

<sup>1</sup>Supplemental Material. Additional information about materials and methods, forward modeling simulations, and data tables. Please visit <https://doi.org/10.1130/GEOL.S.22229644> to access the supplemental material, and contact editing@geosociety.org with any questions.

re-exposure would generate new nuclides at the production value, raising  $^{26}\text{Al}/^{10}\text{Be}$  ratios.

## DISCUSSION

The lengthy intervals of sediment burial suggested by our data are interpreted to indicate persistent Laurentide cover in sediment source areas during most of the last million years. Till could shield bedrock from cosmic radiation, but till only partially covers glaciated regions in North America today (Pelletier et al., 2016). Even if till were present, it too would have been irradiated during ice-free interglacials and then exported when ice readvanced. Alternatively, the sediment we analyzed could have been stored underwater in Hudson Bay and Hudson Strait or on continental shelves for many glacial cycles. However, our samples were derived from quartz-bearing terranes, which are mostly above sea level, while carbonate sediment in Heinrich layers was derived from submerged carbonate outcrops in Hudson Strait and Hudson Bay. Furthermore, the smoothly decreasing trend in  $^{10}\text{Be}$  concentrations in western samples suggests that the sediments we analyzed came from steadily eroding areas and was not extensively mixed and remobilized during transport to the seafloor.

Forward modeling helps to quantify the amount of mid-to-late Pleistocene exposure our data can accommodate and strongly suggests Laurentide ice remained over sediment source areas during most interglacials of the past million years. This model (see the Supplemental Materials) simulates cosmogenic nuclide production in a bedrock profile over the Pleistocene when ice cover is absent; when ice cover is present, production stops, and erosion begins. Nuclides decay continuously with and without ice cover. We ran several ice-cover histories with

different interglacial exposure durations and glacial erosion rates to help bound plausible geologic scenarios. For instance, exposure during every Pleistocene interglacial could have only been on the order of 1–2 k.y.; otherwise, measured  $^{26}\text{Al}/^{10}\text{Be}$  ratios would be closer to the production ratio (Fig. 3, scenario 1). Similar results were found when we limited exposure during the past million years to only marine isotope stages 5e, 9, and 11 (Fig. 3, scenario 2). The data could accommodate longer exposures (~5–10 k.y.) during these few mid-to-late Pleistocene interglacials if there were greater exposure during the early Pleistocene, and if much of the sediment came from very slowly eroding areas where old nuclides were preserved (Fig. 3, scenario 3).

Given the likelihood of sediment mixing, these scenarios represent conservative estimates of ice cover. If our samples are mixtures of sediment from areas with different ice-cover histories, some regions would have even lower  $^{26}\text{Al}/^{10}\text{Be}$  ratios, and thus more persistent ice cover, than assumed in our modeling. The  $^{26}\text{Al}/^{10}\text{Be}$  ratios are more heavily influenced by sediments with higher nuclide concentrations because they contribute more nuclides on a per mass basis. This effect helps to offset the bias of the sediment record toward the most erosive areas such that the  $^{26}\text{Al}/^{10}\text{Be}$  record is more broadly representative of all sediment source regions.

Other lines of evidence are consistent with persistent Laurentide ice during most interglacials. Interglacial sea levels prior to the last interglacial typically were within  $0 \pm 20$  m relative to the present (Past Interglacials Working Group of PAGES, 2016), and remnant ice existed across parts of northeastern Canada (Dalton et al., 2020) in the early Holocene when sea

levels were only 10–20 m below present (Lambeck et al., 2014). Therefore, the lower end of the  $0 \pm 20$  m interglacial sea-level range would be consistent with the survival of some Laurentide ice sectors during interglacial periods. The frequent occurrence of North Atlantic ice-rafted debris within mid-to-late Pleistocene interglacials indicates the presence of marine-terminating ice around the North Atlantic even during warm times; ice-rafted debris is rarely absent from cores taken at locations in the path of Laurentide icebergs near eastern Canada via the Labrador Current and south of Iceland via the North Atlantic Current during the past 750 and 1700 k.y., respectively (McManus et al., 1999; Channell et al., 2012; Barker et al., 2022). Some of the ice-rafted debris peaks along eastern Canada also contain detrital carbonate, suggesting contributions from the Laurentide Ice Sheet (Channell et al., 2012). Although marine  $^{18}\text{O}$  values provide a less direct constraint on global ice volume, interglacials in the LR04  $^{18}\text{O}$  stack (Lisiecki, and Raymo, 2005) reached Holocene levels only a few times during the past 2 m.y. (Fig. 3A).

Our data support previous findings of low  $^{26}\text{Al}/^{10}\text{Be}$  ratios in material from northeastern Canada. Many cosmogenic nuclide measurements of bedrock from Baffin Island and Labrador have low  $^{26}\text{Al}/^{10}\text{Be}$  ratios, similar to our results (Fig. 1), indicating long burial and minimal exposure in some locations underlying the Laurentide Ice Sheet over the last million years (e.g., Miller et al., 2006; Briner et al., 2006, 2014; Corbett et al., 2016). Our ice-rafted debris record provides a more spatially integrated estimate of exposure and erosion history, suggesting that larger areas of northeastern Canada than just the specific landscapes previously studied

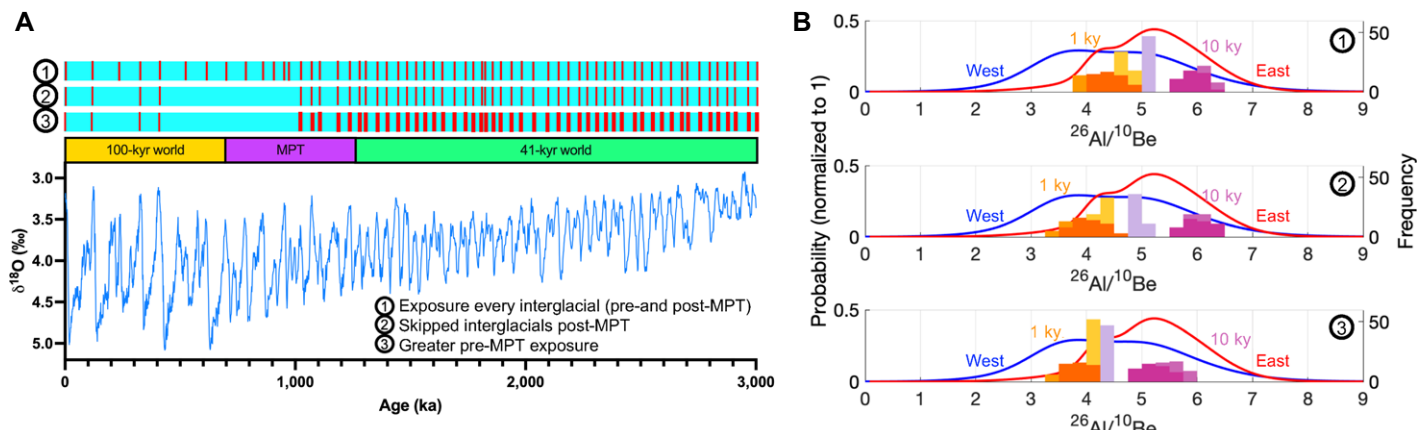


**Figure 3. Modeled and measured  $^{26}\text{Al}/^{10}\text{Be}$  ratios in ice-rafted debris.** (A)  $^{10}\text{Be}$  and  $^{26}\text{Al}$  concentrations simulated for three hypothetical ice-cover scenarios, with interglacial exposures of 1 and 10 k.y. lengths. Scenario 1 has exposure (red bars) during every Pleistocene interglacial. Scenario 2 features exposure during every interglacial until 1 Ma, but only during select interglacials thereafter (marine isotope stages [MIS] 1, 5e, 9, and 11). Scenario 3 is the same as scenario 2, but interglacial exposures are twice as long before 1 Ma as after (i.e., scenarios with 1 k.y. and 10 k.y. exposures after 1 Ma have 2 k.y. and 20 k.y. exposures before 1 Ma). The LR04  $^{18}\text{O}$  stack (Lisiecki and Raymo, 2005) is shown as a proxy for global ice volume. MPT—Mid-Pleistocene Transition. (B) Histograms showing simulated  $^{26}\text{Al}/^{10}\text{Be}$  ratios from 65 ka to 14 ka for 1 k.y. (orange) and 10 k.y. (purple) interglacial exposures using 1, 10, and 100 mm/k.y. (from dark to light shading) subglacial erosion rates. Measured  $^{26}\text{Al}/^{10}\text{Be}$  ratios from the western (blue) and eastern (red) North Atlantic samples are shown as probability distribution functions.

were covered by persistent ice through much of the later Pleistocene, although uncertainties in provenance make it difficult to clearly define the scale of ice cover.

Our data suggest the Laurentide Ice Sheet fully deglaciated only when numerous factors aligned to drive negative surface mass balance for long enough (Ullman et al., 2015). Forcing mechanisms vary among interglacials, such as the phasing of obliquity and precession, greenhouse gas concentrations, and preceding ice-sheet geometry; perhaps only those interglacials with  $\text{CO}_2$  maxima near or above Holocene levels reached the threshold for complete deglaciation. Rather than being prototypical, the interglacial that we find ourselves in today, with little Northern Hemisphere ice outside of Greenland, may be one of a very few such extreme events in the past million years.

## ACKNOWLEDGMENTS

We thank the International Ocean Discovery Program (IODP) Bremen Core Repository (Bremen, Germany), Woods Hole Oceanographic Institution Seafloor Samples Laboratory (Massachusetts, USA), and British Ocean Sediment Core Research Facility (Southampton, UK) for sediment samples. David Hodell, Richard Alley, Tamara Pico, Colin Meyer, Alex Robel, Shaun Marcott, and Luke Zoet provided useful conversations. This research was funded by U.S. National Science Foundation grants NSF-EAR1735676 (to Bierman), ANS-2116208, ANS-2116209 and ANS-2116210, a Purdue Rare Isotope Measurement Laboratory (PRIME Lab) seed grant, and Boston College. This article was prepared in part by Lawrence Livermore National Laboratory staff under contract DE-AC52-07NA27344; LLNL-JRNL-832456.

## REFERENCES CITED

Barker, S., et al., 2022, Persistent influence of precession on northern ice sheet variability since the early Pleistocene: *Science*, v. 376, p. 961–967, <https://doi.org/10.1126/science.abm4033>.

Batchelor, C.L., Margold, M., Krapp, M., Murton, D.K., Dalton, A.S., Gibbard, P.L., Stokes, C.R., Murton, J.B., and Manica, A., 2019, The configuration of Northern Hemisphere ice sheets through the Quaternary: *Nature Communications*, v. 10, 3713, <https://doi.org/10.1038/s41467-019-11601-2>.

Bigg, G.R., Levine, R.C., and Green, C.L., 2011, Modelling abrupt glacial North Atlantic freshening: Rates of change and their implications for Heinrich events: *Global and Planetary Change*, v. 79, p. 176–192, <https://doi.org/10.1016/j.gloplacha.2010.11.001>.

Bond, G., and Lotti, R., 1995, Iceberg discharges into the North Atlantic on millennial time scales during the last glaciation: *Science*, v. 267, p. 1005–1010, <https://doi.org/10.1126/science.267.5200.1005>.

Bond, G., et al., 1992, Evidence for massive discharges of icebergs into the North Atlantic Ocean during the last glacial period: *Nature*, v. 360, p. 245–249, <https://doi.org/10.1038/360245a0>.

Briner, J.P., Gosse, J.C., and Bierman, P.R., 2006, Applications of cosmogenic nuclides to Laurentide ice sheet history and dynamics, in Alonso-Zarza, A.M., and Tanner, L.H., eds., *In Situ-Produced Cosmogenic Nuclides and Quantification of Geological Processes*: Geological Society of America Special Paper 415, p. 29–41, [https://doi.org/10.1130/2006.2415\(03\)](https://doi.org/10.1130/2006.2415(03)).

Briner, J.P., Lifton, N.A., Miller, G.H., Refsider, K., Anderson, R., and Finkel, R., 2014, Using in situ cosmogenic  $^{10}\text{Be}$ ,  $^{14}\text{C}$ , and  $^{26}\text{Al}$  to decipher the history of polythermal ice sheets on Baffin Island, Arctic Canada: *Quaternary Geochronology*, v. 19, p. 4–13, <https://doi.org/10.1016/j.quageo.2012.11.005>.

Briner, J.P., Goehring, B.M., Mangerud, J., and Svendsen, J.I., 2016, The deep accumulation of  $^{10}\text{Be}$  at Utsira, southwestern Norway: Implications for cosmogenic nuclide exposure dating in peripheral ice sheet landscapes: *Geophysical Research Letters*, v. 43, p. 9121–9129, <https://doi.org/10.1002/2016GL070100>.

Channell, J.E.T., Hodell, D.A., Romero, O., Hillaire-Marcel, C., de Vernal, A., Stoner, J.S., Mazaud, A., and Röhl, U., 2012, A 750-kyr detrital-layer stratigraphy for the North Atlantic (IODP Sites U1302–U1303, Orphan Knoll, Labrador Sea): *Earth and Planetary Science Letters*, v. 317–318, p. 218–230, <https://doi.org/10.1016/j.epsl.2011.11.029>.

Corbett, L.B., Bierman, P.R., and Davis, P.T., 2016, Glacial history and landscape evolution of southern Cumberland Peninsula, Baffin Island, Canada, constrained by cosmogenic  $^{10}\text{Be}$  and  $^{26}\text{Al}$ : *Geological Society of America Bulletin*, v. 128, p. 1173–1192, <https://doi.org/10.1130/B31402.1>.

Dalton, A.S., et al., 2020, An updated radiocarbon-based ice margin chronology for the last deglaciation of the North American ice sheet complex: *Quaternary Science Reviews*, v. 234, <https://doi.org/10.1016/j.quascirev.2020.106223>.

Dalton, A.S., Stokes, C.R., and Batchelor, C.L., 2022, Evolution of the Laurentide and Innuitian ice sheets prior to the Last Glacial Maximum (115 ka to 25 ka): *Earth-Science Reviews*, v. 224, <https://doi.org/10.1016/j.earscirev.2021.103875>.

Fendrock, M., Condron, A., and McGee, D., 2022, Modeling iceberg longevity and distribution during Heinrich Events: *Paleoceanography and Paleoclimatology*, v. 37, p. 1–12, <https://doi.org/10.1029/2021PA004347>.

Gosse, J.C., and Phillips, F.M., 2001, Terrestrial in situ cosmogenic nuclides: Theory and application: *Quaternary Science Reviews*, v. 20, p. 1475–1560, [https://doi.org/10.1016/S0277-3791\(00\)00171-2](https://doi.org/10.1016/S0277-3791(00)00171-2).

Groote, P.M., and Stuiver, M., 1999, GISP2 oxygen isotope data: PANGAEA, <https://doi.org/10.1594/PANGAEA.56094>.

Grousset, F.E., Labeyrie, L., Sinko, J.A., Cremer, G., Duprat, J., Cortijo, E., and Huonll, S., 1993, Patterns of ice-rafted detritus in the glacial North Atlantic (40–55°N): *Paleoceanography*, v. 8, p. 175–192, <https://doi.org/10.1029/92PA02923>.

Gwiazda, R.H., Hemming, S.R., and Broecker, W.S., 1996, Provenance of icebergs during Heinrich event 3 and the contrast to their sources during other Heinrich episodes: *Paleoceanography*, v. 11, p. 371–378, <https://doi.org/10.1029/96PA01022>.

Hemming, S.R., 2004, Heinrich events: Massive late Pleistocene detritus layers of the North Atlantic and their global climate imprint: *Reviews of Geophysics*, v. 42, RG1005, <https://doi.org/10.1029/2003RG000128>.

Hemming, S.R., and Hajdas, I., 2003, Ice-rafted detritus evidence from  $^{40}\text{Ar}/^{39}\text{Ar}$  ages of individual hornblende grains for evolution of the eastern margin of the Laurentide ice sheet since 43  $^{14}\text{C}$  ky: *Quaternary International*, v. 99–100, p. 29–43, [https://doi.org/10.1016/S1040-6182\(02\)00110-6](https://doi.org/10.1016/S1040-6182(02)00110-6).

Hemming, S.R., Broecker, W.S., Sharp, W.D., Bond, G.C., Gwiazda, R.H., McManus, J.F., Klas, M., and Hajdas, I., 1998, Provenance of Heinrich layers in core V28-82, northeastern Atlantic:  $^{40}\text{Ar}/^{39}\text{Ar}$  ages of ice-rafted hornblende, Pb isotopes in feldspar grains, and Nd-Sr-Pb isotopes in the fine sediment fraction: *Earth and Planetary Science Letters*, v. 164, p. 317–333, [https://doi.org/10.1016/S0012-821X\(98\)00224-6](https://doi.org/10.1016/S0012-821X(98)00224-6).

Kleman, J., Jansson, K., de Angelis, H., Stroeve, A.P., Hättestrand, C., Alm, G., and Glasser, N., 2010, North American ice sheet build-up during the last glacial cycle, 115–21 kyr: *Quaternary Science Reviews*, v. 29, p. 2036–2051, <https://doi.org/10.1016/j.quascirev.2010.04.021>.

Lambeck, K., Rouby, H., Purcell, A., Sun, Y., and Cambridge, M., 2014, Sea level and global ice volumes from the Last Glacial Maximum to the Holocene: *Proceedings of the National Academy of Sciences of the United States of America*, v. 111, p. 15,296–15,303, <https://doi.org/10.1073/pnas.1114762111>.

Lisiecki, L.E., and Raymo, M.E., 2005, A Pliocene–Pleistocene stack of 57 globally distributed benthic  $\delta^{18}\text{O}$  records: *Paleoceanography*, v. 20, PA1003, <https://doi.org/10.1029/2004PA001071>.

Mao, L., Piper, D.J.W., Saint-Ange, F., Andrews, J.T., and Kienast, M., 2014, Provenance of sediment in the Labrador Current: A record of hinterland glaciation over the past 125 ka: *Journal of Quaternary Science*, v. 29, p. 650–660, <https://doi.org/10.1002/jqs.2736>.

McManus, J.F., Oppo, D.W., and Cullen, J.L., 1999, A 0.5-million-year record of millennial-scale climate variability in the North Atlantic: *Science*, v. 283, p. 971–975, <https://doi.org/10.1126/science.283.5404.971>.

Miller, G.H., Briner, J.P., Lifton, N.A., and Finkel, R.C., 2006, Limited ice-sheet erosion and complex exposure histories derived from in situ cosmogenic  $^{10}\text{Be}$ ,  $^{26}\text{Al}$ , and  $^{14}\text{C}$  on Baffin Island, Arctic Canada: *Quaternary Geochronology*, v. 1, p. 74–85, <https://doi.org/10.1016/j.quageo.2006.06.011>.

Miller, G.H., et al., 2022, Last interglacial lake sediments preserved beneath Laurentide and Greenland ice sheets provide insights into Arctic climate amplification and constrain 130 ka of ice-sheet history: *Journal of Quaternary Science*, v. 37, p. 979–1005, <https://doi.org/10.1002/jqs.3433>.

Past Interglacials Working Group of PAGES, 2016, Interglacials of the last 800,000 years: *Reviews of Geophysics*, v. 54, p. 162–219, <https://doi.org/10.1002/2015RG000482>.

Pelletier, J.D., Broxton, P.D., Hazenberg, P., Zeng, X., Troch, P.A., Niu, G., Williams, Z.C., Brunke, M.A., and Gochis, D., 2016, Global 1-km Gridded Thickness of Soil, Regolith, and Sedimentary Deposit Layers: Oak Ridge, Tennessee, Oak Ridge National Laboratory Distributed Active Archive Center, <https://doi.org/10.3334/ORNLDAC/1304>.

Ruddiman, W.F., 1977, Late Quaternary deposition of ice-rafted sand in the subpolar North Atlantic (lat 40° to 65°N): *Geological Society of America Bulletin*, v. 88, p. 1813–1827, [https://doi.org/10.1130/0016-7606\(1977\)88<1813:LQDOIS>2.0.CO;2](https://doi.org/10.1130/0016-7606(1977)88<1813:LQDOIS>2.0.CO;2).

Ullman, D.J., Carlson, A.E., Anslow, F.S., Legrande, A.N., and Licciardi, J.M., 2015, Laurentide ice-sheet instability during the last deglaciation: *Nature Geoscience*, v. 8, p. 534–537, <https://doi.org/10.1038/ngeo2463>.

Printed in USA